MRS Communications (2023) 13:1266–1274

https://doi.org/10.1557/s43579-023-00436-0

MRS Communications

Research Letter

On the direct ink write (DIW) 3D printing of styrene-butadiene rubber (SBR)-based adhesive sealant

Vincent Joseph Garcia, Department of Chemical and Biomolecular Engineering, Department of Materials Science and Engineering, Department of Mechanical, Aerospace, and Biomedical Engineering, Institute for Advanced Materials and Manufacturing, University of Tennessee, Knoxville, TN 37996, USA
G. M. Fazley Elahee, Department of Macromolecular Science and Engineering, Case Western Reserve University, Cleveland, OH 44106, USA; Novaguard Solutions, Cleveland, OH 44114, USA
Alvin Kim Collera, Materials Science Division, Department of Science and Technology, Industrial Technology Development Institute, 1631 Taguig, Philippines
Travis Thornton, Department of Chemical and Biomolecular Engineering, Department of Materials Science and Engineering, Department of Mechanical, Aerospace, and Biomedical Engineering, Institute for Advanced Materials and Manufacturing, University of Tennessee, Knoxville, TN 37996, USA
Xiang Cheng, Department of Macromolecular Science and Engineering, Case Western Reserve University, Cleveland, OH 44106, USA
Salvador Rohan, Emmaline L. Howard, and Alejandro H. Espera Jr., Department of Chemical and Biomolecular Engineering, Department of Materials Science and Engineering, Department of Mechanical, Aerospace, and Biomedical Engineering, Institute for Advanced Materials and Manufacturing, University of Tennessee, Knoxville, TN 37996, USA
Rigoberto C. Advincula, Department of Chemical and Biomolecular Engineering, Department of Materials Science and Engineering, Department of Mechanical, Aerospace, and Biomedical Engineering, Institute for Advanced Materials and Manufacturing, University of Tennessee, Knoxville, TN 37996, USA; Department of Macromolecular Science and Engineering, Case Western Reserve University, Cleveland, OH 44106, USA; Center for Nanophase Materials Sciences, Oak Ridge National Laboratory, Oak Ridge, TN 37830, USA

Address all correspondence to Rigoberto C. Advincula at **radvincu@utk.edu**

(Received 4 June 2023; accepted 10 August 2023; published online: 22 August 2023)

Abstract

Direct Ink Writing (DIW) utilizes a wide range of ink formulations to produce desirable 3D-printed structures and properties. Styrene-butadiene rubber (SBR) is an attractive candidate for 3D printing owing to its commercial availability, rheology, excellent mechanical properties, good impact resilience, and chemical stability. The SBR-based sealant was 3D printed in a DIW process, even in an ambient environment. The rheological behavior was assessed and correlated with optimized printing parameters. Important physico-chemical properties of the 3D-printed material were reported showing excellent properties as an elastomer. This work should expand the potential applications of existing rubber-based materials in additive manufacturing.

Introduction

Additive manufacturing (AM) has accumulated increasing research interest since its emergence a few decades ago. AM transforms a virtual design into three-dimensional structures by adding material in a layer-by-layer fashion. AM also known as 3D printing can provide cost-efficient solutions even for applications demanding high design complexity.[1,2] Among these techniques, Direct Ink Writing (DIW) is one of the most widely used, highly versatile extrusion-based AM techniques from viscous formulations resulting in 3D-printed structures with desirable tailored properties.[3] Despite DIW's advantages, the resulting mechanical integrity of the fabricated functional parts is still inadequate, limiting its potential end use in industrial applications.[4,5]

Synthetic rubber materials, such as styrene-butadiene rubbers (SBR), which is a copolymer of butadiene and styrene typically produced either via solution polymerization or emulsion polymerization,[6] can offer excellent mechanical properties, very high elongation at break, good impact resilience, and good chemical stability. They are popular materials in rubber manufacturing industries for automotive, construction, and even protective clothing.[7] However, fabrication requirements such as high-temperature and pressure processes pose challenges for these materials for AM applications.

Caulking agents or adhesive sealants are typically used to fill cracks and gaps on various surfaces or as bonding agents between joints. Many options are available for the intended application. Among these, commercially available rubber-based sealants that readily cure at room temperature are potential candidates for DIW 3D printing. They can be resilient in applications requiring expansion and contraction, such as exterior joints or even in adverse weather conditions where it stretches and recovers quickly without breaking.[8] There are a number of formulations based on acrylates, silicones, polyurethanes, and SBR matrices for preparing commercially available sealants. This work aims to demonstrate the viability of utilizing synthetic SBR rubber-based sealants as feedstock for DIW 3D printing. The copolymer rubber sealant is combined with a solvent to produce a gel-like consistency that cures through the evaporation of the solvent upon its release from the cartridge, allowing it to behave as an elastomeric rubber even at room temperature.[9] Rheological properties for DIW 3D printing

Rigoberto Advincula was an editor of this journal during the review and decision stage. For the MRS Communications policy on review and publication of manuscripts authored by editors, please refer to http://www.mrs.org/editormanuscripts/.

and various physico-chemical performance properties of the 3D-printed parts, such as their mechanical, thermal, and electrical, show excellent properties for future applications. The role of additives on these formulations are also discussed.

Materials and methods

Materials

A commercially available clear Lexel®, which is a synthetic copolymer of SBR-based sealant formulation [Fig. 1(a, b)] was used. It is a super-elastic, super-adhesive, and paintable sealant that seals around tubs, sinks, countertops, window frames, and door frames, as described by its manufacturer. It could also be applied to wet or dry surfaces indoors or outdoors; it is tough and can withstand about 400% joint movement. The manufacturer also claimed that the clear sealant is 19 times clearer than silicone and does not discolor or cloud up over time.[10]

Methodology

3D printing was done on a Hyrel Hydra 16a with an engine SR with SDS 30XT modular printing head and 30-mL syringes to 3D print the material. Material composition characterization was performed by Pyrolysis–gas chromatography–mass spectrometry (Py-GC/MS) involving evolved gas analysis (EGA) and flash pyrolysis. Fourier Transform infrared spectroscopy (FTIR) was used to identify the organic functional groups present in the sample. Thermogravimetric analysis (TGA) was performed to assess the sample's thermal behavior and relative composition. The differential thermogravimetric (DTG) ratio was obtained by taking the first derivative of the TGA. The morphology of the 3D-printed specimens was characterized using scanning electron microscopy (SEM). The rheological behavior of the ink was evaluated using a parallel plate rheometer. Finally, various mechanical, thermal, and electrical properties of the 3D-printed parts were also assessed. A detailed description of each characterization, the methods or equipment used, and the optimized 3D printing parameter is available in the Supplementary Information (SI) document.

Results and discussion

Rheology

The rheology of the ink plays a vital role in DIW 3D printing. A thixotropic property is necessary for materials intended to be used for this technique, where the ink should exhibit a shear-thinning behavior by which a progressive reduction in the apparent viscosity of the material is observed through time as constant shear stress is applied during the extrusion. It is then followed by a gradual recovery of the material after removing the applied stress, giving the ink the ability to hold its desired shape upon extrusion. The thixotropy of an adhesive material may be observed by plotting its storage modulus (G') and loss modulus (G'') versus its oscillation strain, per ASTM D2556-14. This G' and G'' versus oscillation strain curve for Lexel® is presented in Fig. 1(c). It can be observed from Fig. 1(c) that the initial G' values are above or more significant than G'' along the linear viscoelastic (LVE) regime, which suggests that it exhibits a shear-thinning behavior, indicating that the sealant becomes less viscous and can flow upon application of shear stress. This transition from a

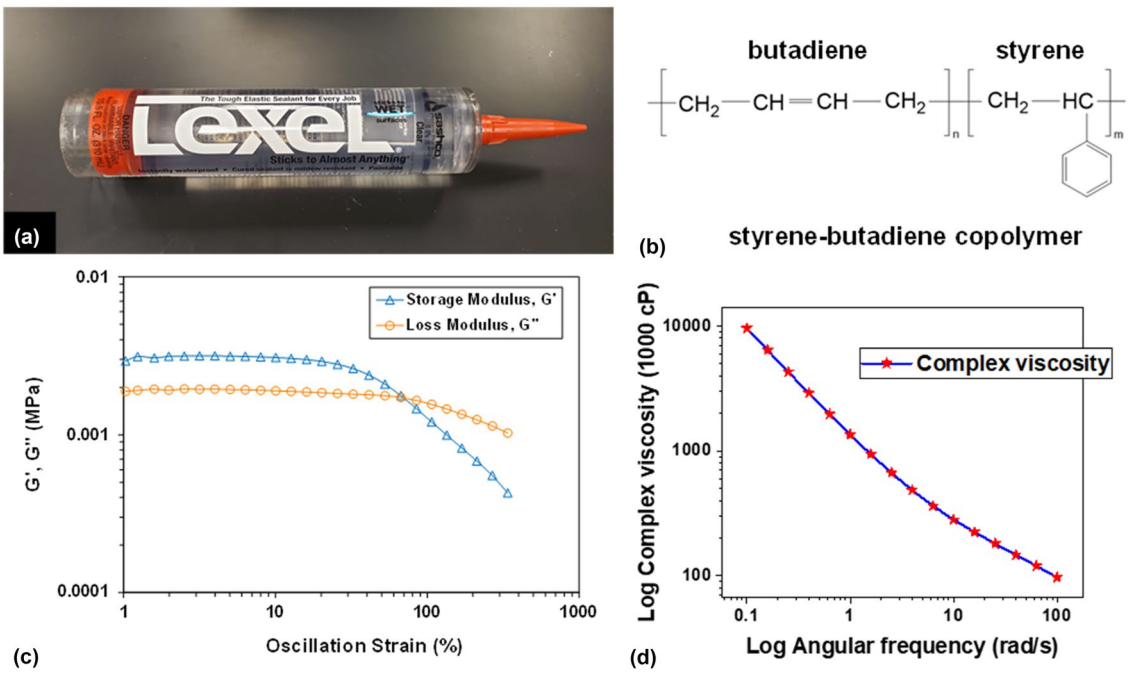

Figure 1. (a) Commercially available SBR Lexel®, (b) chemical structure of styrene-butadiene rubber, (c) storage modulus (G′) and loss modulus (G″) versus oscillation strain curve, (d) and complex viscosity versus angular frequency curve.

gel-like material to a more flowable substance is evidenced by the point of intersection or cross-over between storage and loss moduli at the end of the linear of the viscoelastic (EVLE) regime as shown in Fig. 1(c). This is also considered the yield stress at which this phenomenon occurs. The complex viscosity versus angular frequency curve of the analysis is also shown in Fig. 1(d), which displays the decreasing viscosity of the sealant as the shear rate increases, thus also suggesting the shear-thinning behavior.[11,12] All these indicates that the sealant is viable as a viscoelastic 3D printing ink for the DIW technique.

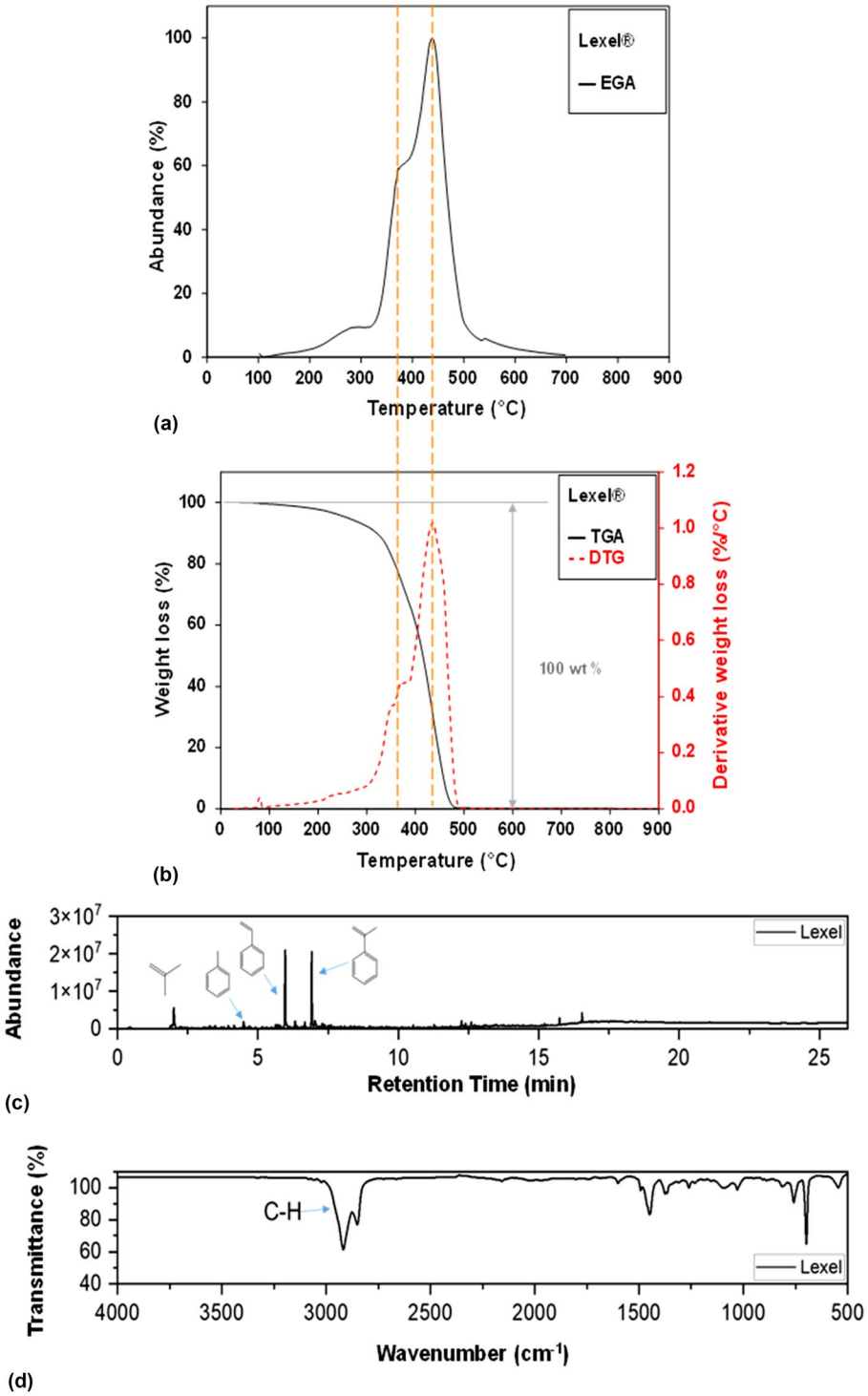

Figure 2. (a) EGA and (b) TGA curves, (c) flash pyrolysis chromatogram, and (d) FTIR spectra of the sample.

Evolved gas analysis and thermogravimetric analysis

Figure 2(a, b) shows the EGA and TGA curves. A two-part degradation at a temperature range of 200 to 500°C is demonstrated in Fig. 2(a), which implies that the sample is a two-part copolymer, as described by the manufacturer. The TGA and DTG profile are shown in Fig. 2(b). The TGA curve shows a single major degradation step as correlated by the presence of a single peak in its corresponding DTG profile. The single-step degradation, which started from about 300 to 500°C, suggests a 100% weight decomposition of the copolymer material. The absence of any solid or mineral component (inorganic additives) with this formulation is evidenced by the complete degradation or weight loss at about 480°C. In some sealant or adhesive formulations, inorganic or mineral additives are used to support rheological properties, densification, and thermal stability. Similar results in temperature range and degradation were also obtained from the studies of Castaldi et al. and Shield et al. which confirm that the sample is SBR based.[13,14]

Pyrolysis–gas chromatography–mass spectrometry and Fourier transform infrared spectroscopy

Figure 2(c) displays the flash pyrolysis chromatogram of the sealant. The observed peaks resulting from the flash pyrolysis single shot at 500°C indicate the presence of isobutene and styrene/α-methyl styrene, which confirms that the copolymer is an SBR material. The presence of toluene as the solvent was also confirmed, as declared by the manufacturer. A solid characteristic broad peak of the C–H bond in the range of ~2800 to 3000 cm^{-1}[15] was observed in the FTIR spectra as shown in Fig. 2(d), which corroborates the result of the Py-GC/MS mass spectral analysis. Another, consideration is the absence of plasticizer additives which is sometimes added to improve the flow behavior with application. These composition verification along with thermal analysis indicates that the formulation as it is is mostly SBR copolymer material with very good rheological behavior but may have limited thermal stability. This indicates the possibility for future repurposing of this base formulation with different additives.

Direct ink write 3D printing

DIW technique produced 3D-printed structures of the SBR polymer sealant as its ink. The images of the 3D-printed objects with simple and complex designs, such as long bars, tensile bars, and flower structures, are shown in Fig. 3(a–c). The successful fabrication of these parts demonstrates the ability of DIW to utilize commercially available synthetic rubber-based materials to produce geometrically and structurally complex 3D-printed objects with high printing resolution

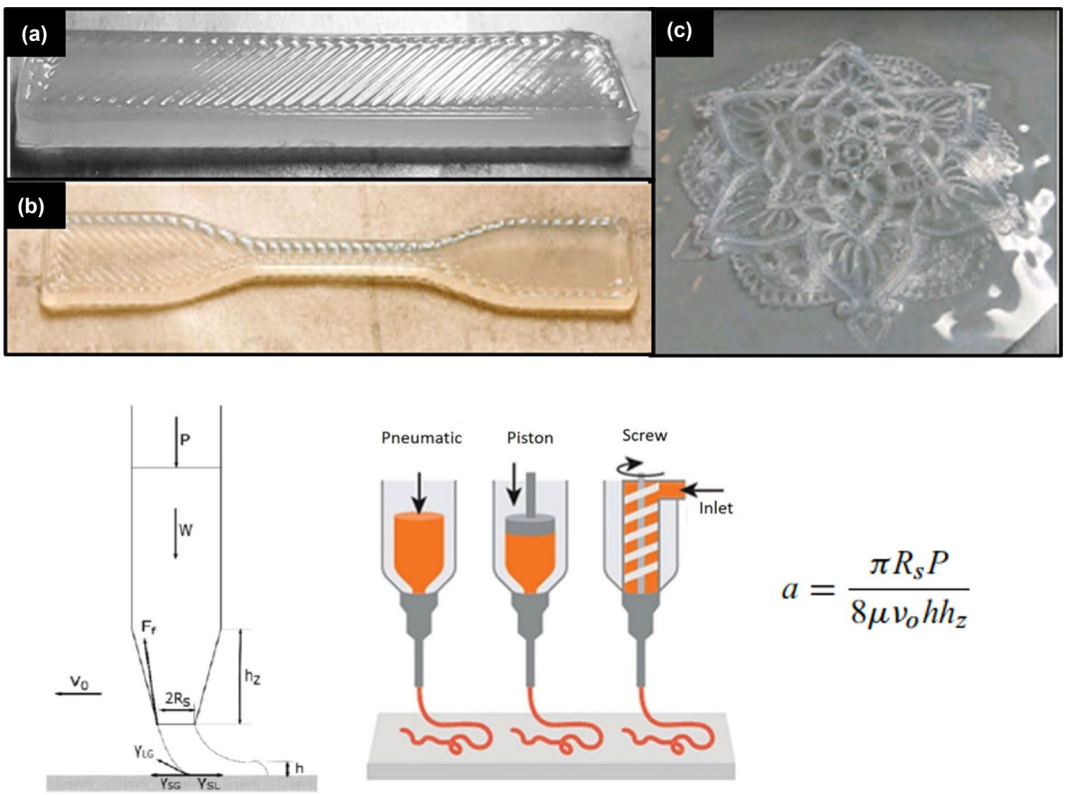

Figure 3. DIW 3D-printed (a) long bar, (b) tensile bar, and (c) flower structure using the SBR-based sealant as ink and (d) a dynamic fluid model that can be modeled after extruding materials from a syringe onto a flat substrate with good adhesion to the ink.

and quality. In a previous report by Kamath et al. the 3D printing of SBR rubber was achieved using a formulated ink or liquid SBR with rheological modifiers, vulcanizing agents, activators, and other additives.[16] That work actually required a vulcanization step before it can provide a useful thermo-mechanical property. The properties were reported which showed its dependence on the curing time/temperature and also the role of each additive from rheology and then curing. In our case, we directly used a commercially available sealant SBR material which we deconstructed using IR, pyrolysis GC/MS, and other characterization methods to correlate properties with composition. This is different from the previous work in that the yield stress and storage modulus requirements for 3D printability is achieved by evaporation of the solvent with extrusion and printing layer by layer. In principle, the optimization process of the 3D printability can be carried out by similar studies done with acrylate- and silicone-based sealants.[17,18] With good adhesion of the viscous ink to the substrate, a simplistic dynamic fluid model can be used to simulate relationships between how the viscosity of the fluid (μ), the internal radius of the nozzle (Rs), print speed (vo), the height of the printed pattern (h), tapered zone length (hz), and driving pressure (P) can affect the width of deposited fluid (a) as shown in Eq. 1 and Fig. 3.

$$a = \frac{\pi R_s P}{8\mu v_o h h_z}. \quad (1)$$

Scanning electron microscopy

Morphological characterization of the 3D-printed sample was performed using SEM. The SEM images of the surface of the 3D-printed sample are shown in Fig. 4(a, b). A relatively uniform surface can be observed from the micrographs having areas with scale-like features, which the manufacturer described since Lexel® develops a dirt-resistive skin upon the solvent's evaporation just minutes after the sealant's application.[9] The aging studies and volume stability in shrinkage were monitored and is discussed in a later section as shown in Fig. 4(c, d). The lack of any solid additives also support these almost featureless and uniform morphology.

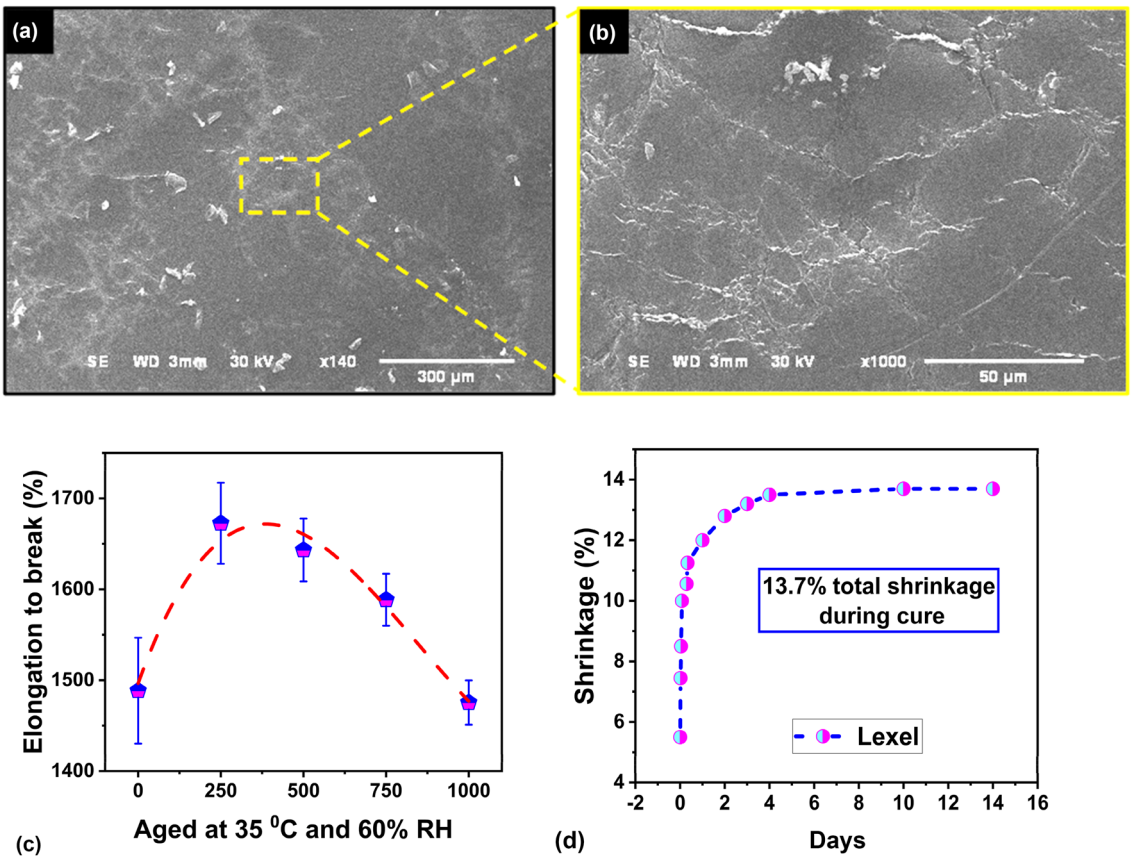

Figure 4. SEM images of the 3D-printed sample at (a) ×140 and (b) ×1000 magnification. Aging and curing/volume change studies: (c) Impact on tensile elongation over aging at 35°C and 60% RH and (d) Shrinkage during cure at room temperature as a function of days.

Mechanical properties

Tensile testing

Tensile specimens were printed based on ASTM D412 specifications to evaluate the mechanical properties. The obtained value of yield strength, ultimate tensile strength, and elastic modulus are 674 Pa, 645.3 psi (~4.45 MPa), and 320 Pa, respectively, while the elongation at break reached about 1307%. The low value obtained for the yield strength and ultimate tensile strength is expected of a rubber material. The significant value of the maximum strain experienced is attributed to the styrene-butadiene copolymer composition of the sealant, which is crosslinked linearly. Previous report on tensile properties of another SBR material showed tensile values of 2.11 MPa and elongation at break up to 400%.[16] This property was achieved with curing/vulcanization of the formulated L-SBR up to 160°C which was not necessary with this room-temperature SBR sealant. In this case, the room-temperature 3D-printed SBR sealant showed longer elongation at break compared to the high-temperature crosslinked L-SBR.

Compression deflection test

Compression tests at 10 and 30% deflection were performed following the ASTM D575. Low values of compressive stresses of 0.03 and 0.13 MPa were obtained at 10 and 30% deflection, respectively. A previous study by Elahee et al. on the 3D printing of acrylic sealants attributed the low values of compressive stresses obtained to the small number of fillers present in the acrylic sealant, providing insufficient impact-resisting changes to compression deflection. As mentioned earlier, SBR copolymer composition without any other filler presents results in the low compressive stress values obtained in this test.[17,18] Additionally, no plastic deformation was observed at 10% deflection. In comparison, a small plastic deformation of about 2.3% at 30% deflection was experienced, most likely due to the tear in the longitudinal crosslink network of the elastomeric polymer matrix of the sealant.

Durometer hardness test

The 3D-printed samples were subjected to durometer hardness testing after being cured for at least a week and exposed to room temperature open air. Hardness measurement is performed to measure the resistance of a material to mechanical indentation. The obtained Shore A hardness value of 30 is relatively low, indicating that this type of rubber is considered soft.

Electrical properties

Dielectric constant measurement

The dielectric constant of a material is the amount of electric potential energy in the form of induced polarization that can be stored in each volume of the material in the presence of an electric field.[19] The measured dielectric constant at 50 kHz and 1 V is 1.74. A low dielectric constant suggests that the SBR sealant can prevent localized heating upon exposure to a high-voltage electric field.

Dissipation factor

The reciprocal of the ratio between the capacitive reactance of an insulating material and its resistance at a specified frequency is called its dissipation factor. Essentially, it is defined as the ratio between the permittivity and the conductivity of an electrically insulating material. It measures the energy absorbed or dissipated by the material upon application of an electric field due to the internal motion in the material. Measurement of the dissipation factor is significant in applications, such as encapsulation of electric components and wiring insulation in high-performance electronic systems and plastic insulation for high-frequency applications, like radar equipment or microwave components.[20,21] The obtained dissipation factor at 50 kHz is 0.000367, which is an extremely low value, indicating its potential as a candidate material for the abovementioned applications.

Breakdown voltage

The maximum voltage an insulating material can withstand before experiencing a catastrophic decrease in resistance resulting in the electrical breakdown that renders the material electrical is called the breakdown voltage. The breakdown strength of a material is vital in applications prone to experiencing voltage surges, such as transformers, circuit breakers, and semiconductors. The extent of crosslinking in the polymer could be correlated with the breakdown voltage, as it is affected by the material's structure.[20,22,23] A relatively high breakdown voltage value of 14.97 kV/mm was observed, which could be likely due to the high linear crosslink density of the copolymer in the sealant. This suggests that the sealant could be a good material for the abovementioned applications.

Volume resistivity

The fundamental material property determining how strongly a material resists the flow of electric current is called volume resistivity. It is essentially the reciprocal of the electrical conductivity of a material. Generally, materials exhibiting volume resistivity above 10^5 Ω-cm are considered electrically insulating; the higher the resistivity, the stronger it resists the flow of electric current, and the less conductive the material becomes.[24–26] The volume resistivity obtained is 1.95×10^{16} Ω-cm, likely due to the high linear crosslink density attained from the intimate densification of polymer chain network as the interstitial solvent molecule evaporates during curing, providing a less free path for charged carriers to flow through it. The

Table I. Average peel adhesion strength on various substrates.

Substrate	Average peel force (lb-f/in)
Stainless steel	21.63
Polyvinyl chloride (PVC)	24.52
Acrylonitrile butadiene styrene (ABS)	23.78
FR4	23.84
Glass	24.2

high-volume resistivity makes it a good material for applications dealing with high voltages and frequencies.

Thermal properties

The thermal properties were investigated by measuring its response to heat application. The measure of the ability of a material to transfer heat is called thermal conductivity. Moreover, it measures the rate at which heat flows through the material.[27] The measured thermal conductivity is 0.14 W/mK which is an extremely low value, represented by the neat polymer matrix where no transport medium for phonon particles to cross the boundary. Thermal diffusivity is another thermal property that measures the rate at which a temperature disturbance travels from one point to another in a material. The obtained thermal diffusivity is 0.10 mm^2/s. Lastly, the specific heat of the sealant was also evaluated, having a value of 1370 J/kgK. This property pertains to the amount of heat necessary to raise the temperature of one kilogram of material by one Kelvin.[27] These values are expected of polymeric materials as they are generally considered thermally insulative.

Peel adhesion strength

Peel adhesion strength measures the force required to remove material from a substrate. The average peel adhesion strength on different substrates is presented in Table I.

Among the various substrates, adhesion on a polyvinyl chloride (PVC) substrate yielded the highest average value of about 24.52 lb-f/in. In comparison, adhesion on a stainless-steel substrate had the lowest average value of approximately 21.63 lb-f/in. The obtained peel force strength data are of high values implying that the sealant has excellent surface adhesion on the tested substrates. The excellent surface adhesion property may be attributed to good interfacial bonding between the SBR copolymer matrix and the substrate compatibility and the high crosslink density or crosslink strength within the SBR-based adhesive matrix.[28] Additionally, the obtained values are similar to those published by the manufacturer, reinforcing their claim that the sealant adheres to most building materials.[9] This indicates that a 3D-printed SBR sealant formulation adheres to a wide range of surfaces enabling multimaterial deposition and geometries of a substrate.[16]

Curing/shrinkage and aging properties

DIW 3D-printed tensile bars were cured for 7 days before being aged at 35°C and 60% RH. At 250-h intervals, five tensile samples were taken out to test for their mechanical properties until 100 h, as shown in Fig. 4(c). The data indicate that after initial 250 h of aging, the crosslink network advanced further beyond the initial 7 days at room temperature reflecting higher elongation and increased elasticity before the break. However, additional aging resulted in oxidative degradation and moisture absorption at the surface and progressively migrated inward with developing brittleness, losing the modulus of elasticity, evidenced by an obvious declining trend of % elongation.[29] The dimensional stability of the 3D-printed 20-cm rectangular part was physically measured at various time intervals for 14 days. Percent length change over days, Fig. 4(d), revealed a total shrinkage during cure was 13.7%. The cause of shrinkage is mainly due to the solvent, toluene, evaporation, and increasing crosslink density over time.[30] Previous studies on a high-temperature vulcanized SBR showed good dimensional accuracy and stability of up to 5.89% which can differentiate the effect of vulcanization on 3D-printed LSBR.[16] These changes can be compensated by accounting for this volume shrinkage and the necessity to adjust infill density. Reports on Vat Photopolymerization of SBR latex elastomers present with acrylate resin crosslinking show versatility in maintaining thermo-mechanical properties and decoupling with DIW methods. These can create new properties in combination with other resins to result in new applications, such as degradable scaffolds.[31,32]

Conclusion

This work reported the necessary viscoelastic and rheological behavior that make the readily and commercially available SBR copolymer sealant viable for DIW 3D printing technique. The 3D printing of simple and complex structures supports this claim. Furthermore, the evaluated properties of the 3D-printed parts, such as their mechanical, electrical, and thermal properties, exhibited results expected of SBR materials upon curing. It also differentiates properties from high-temperature cured and crosslinked LSBR. It is important to do these detailed studies on a readily available material for viability in scale-up of DIW inks. Recommendations for future studies may involve tailoring properties by adding different fillers, such as carbon nanomaterials and graphene oxide, to enhance their thermal and electrical properties with the perspective of using similar protocols for property validation and specific applications.

Acknowledgments

We acknowledge technical support from Frontier Laboratories and Quantum Analytics for technical support. This work (or part of this work) was conducted in Oak Ridge National Laboratory Center for Nanophase Materials Sciences by Rigoberto C. Advincula, a US Department of Energy Office of Science User Facility.

Funding

This study was funded by U.S. Department of Energy.

Data availability

All data for the work are either included in this manuscript or are part of the Electronic Supplementary Information file.

Declarations

Conflict of interest

The authors declare no known conflict of interest or personal relationships that could have appeared to influence the work reported in this paper.

Supplementary Information

The online version contains supplementary material available at https://doi.org/10.1557/s43579-023-00436-0.

References

1. T. McCue, Wohlers Report 2018: 3D Printer industry tops $7 billion, 2018. Available at: https://www.forbes.com/sites/tjmccue/2018/06/04/wohlers-report-2018-3d-printer-industry-rises-21-percent-to-over-7-billion/#577ed47a2d1a. Accessed 15 Oct 2022
2. E.-H. Ramírez-Soria, J. Bonilla-Cruz, M.G. Flores-Amaro, V.J. Garcia, T.E. Lara-Ceniceros, F.E. Longoria-Rodríguez, P. Elizondo, R.C. Advincula, On the effect of ultralow loading of microwave-assisted bifunctionalized graphene oxide in stereolithographic 3D-printed nanocomposites. ACS Appl. Mater. Interfaces. **12**(43), 49061–49072 (2020). https://doi.org/10.1021/acsami.0c13702
3. E.B. Caldona, J.R.C. Dizon, R.A. Viers, V.J. Garcia, Z.J. Smith, R.C. Advincula, Additively manufactured high-performance polymeric materials and their potential use in the oil and gas industry. MRS Commun. **11**(6), 701–715 (2021). https://doi.org/10.1557/s43579-021-00134-9
4. I. Gibson, D.W. Rosen, B. Strucker, *Additive manufacturing technologies: rapid prototyping to direct digital manufacturing*, 2nd edn. (Springer Science+Business Media, LLC, New York, 2010)
5. J.A. Lewis, Direct ink writing of 3D functional materials. Adv. Funct. Mater. **16**(17), 2193–2204 (2006). https://doi.org/10.1002/adfm.200600434
6. R.J. Dhanorkar, S. Mohanty, V.K. Gupta, Synthesis of functionalized styrene butadiene rubber and its applications in SBR-silica composites for high-performance tire applications. Ind. Eng. Chem. Res. **60**(12), 4517–4535 (2021). https://doi.org/10.1021/acs.iecr.1c00013
7. S. Thomas, R. Stephen, *Rubber nanocomposites: preparation, properties and applications* (John Wiley & Sons (Asia) Pte. Ltd., Singapore, 2010)
8. M. Hirsch, Discover the flexibility of caulks and sealants, 2019. Available at: https://knowledge.ulprospector.com/9377/pc-discover-the-flexibility-of-caulks-and-sealants/. Accessed 01 Feb 2023
9. Con-Spec Industries, Lexel is better than silicone, 2013. Available at: https://www.conspecindustries.com/wp-content/uploads/2013/03/lexel.pdf. Accessed 20 Feb 2023
10. Sashco, Lexel technical data sheet (2022), https://sashcoinc.app.box.com/s/unh5zcyega0uimu3c70q6ipizz4m26xa. Accessed 20 Feb 2023
11. Z.J. Smith, D.R. Barsoum, Z.L. Arwood, D. Penumadu, R.C. Advincula, Characterization of micro-sandwich structures via direct ink writing epoxy based cores. J. Sandw. Struct. Mater. **25**(1), 112–127 (2023). https://doi.org/10.1177/10996362221118329
12. D.B. Gutierrez, E.B. Caldona, Z. Yang, X. Suo, X. Cheng, S. Dai, R.D. Espiritu, R.C. Advincula, 3D-printed PDMS-based membranes for CO_2 separation applications. MRS Commun. **12**(6), 1174–1182 (2022). https://doi.org/10.1557/s43579-022-00287-1
13. M.J. Castaldi, E. Kwon, Thermo-gravimetric analysis (TGA) of combustion and gasification of styrene-butadiene copolymer (SBR). Proceedings of the 13th annual North American waste-to-energy conference. Am. Soc. Mech. Eng. (2005). https://doi.org/10.1115/NAWTEC13-3149
14. S.R. Shield, G.N. Ghebremeskel, C. Hendrix, Pyrolysis–GC/MS and TGA as tools for characterizing blends of SBR and NBR. Rubber Chem. Technol. **74**(5), 803–813 (2001). https://doi.org/10.5254/1.3547654
15. A. Nandiyanto, R. Oktiani, R. Ragadhita, How to read and interpret FTIR spectroscope of organic material. Indones. J. Sci. Technol. **4**(1), 97–118 (2019). https://doi.org/10.17509/ijost.v4i1.15806
16. S.S. Kamath, J.W. Choi, 3D printing of synthetic rubber ink via the direct ink writing process. Rubber World **11**, 40–45 (2021)
17. G.M.F. Elahee, L. Rong, C. Breting, J. Bonilla-Cruz, T.E. Lara-Ceniceros, Z.J. Smith, J. Ge, X. Cheng, M. Xu, M. Yang, E.L. Ribeiro, E.B. Caldona, R.C. Advincula, Acrylic sealants as practicable direct ink writing (DIW) 3D-printable materials. MRS Commun. (2023). https://doi.org/10.1557/s43579-023-00343-4
18. A. Espera, J. Dizon, A. Valino, Q. Chen, I. Silva, S. Nguyen, L. Rong, R. Advincula, On the 3D printability of silicone-based adhesives via viscous paste extrusion. MRS Commun. **13**, 102–110 (2023). https://doi.org/10.1557/s43579-022-00318-x
19. D.J. Bergman, The dielectric constant of a composite material—a problem in classical physics. Phys. Rep. **43**(9), 377–407 (1978). https://doi.org/10.1016/0370-1573(78)90009-1
20. J. Bicerano, *Prediction of polymer properties*, 3rd edn. (Marcel Dekker, Inc., New York, 2002)
21. Paul Martin, Dissipation factor of plastic materials explained, 2022. Available at: https://passive-components.eu/dissipation-factor-of-plastic-materials-explained/#:~:text=Dissipation%20Factor%20is%20a%20dimensionless,radar%20equipment%20or%20microwave%20parts. Accessed 04 March 2023
22. P. Barber, S. Balasubramanian, Y. Anguchamy, S. Gong, A. Wibowo, H. Gao, H.J. Ploehn, H.-C. Zur Loye, Polymer composite and nanocomposite dielectric materials for pulse power energy storage. Materials **2**(4), 1697–1733 (2009). https://doi.org/10.3390/ma2041697
23. J. Artbauer, Electric strength of polymers. J. Phys. D: Appl. Phys. **29**(2), 446–456 (1996). https://doi.org/10.1088/0022-3727/29/2/024
24. ASTM D257-14, Standard test methods for DC resistance or conductance of insulating materials, ASTM International, West Conshohocken, PA. (2021). https://doi.org/10.1520/D0257-14R21E01
25. M. Lisowski, Issues of volume resistivity measurement of flat dielectric specimens and evaluation on uncertainty of the measurement results by approximate method at confidence level of 0.95. Metrol. Meas. Syst. **16**(2), 233–248 (2009)
26. S.M. Aharoni, Electrical resistivity of a composite of conducting particles in an insulating matrix. J. Appl. Phys. **43**(5), 2463–2465 (1972). https://doi.org/10.1063/1.1661529
27. W.D. Callister Jr., D.G. Rethwisch, *Materials science and engineering*, 9th edn. (John Wiley & Sons, Inc., USA, 2014)
28. A. Abdel-Hakim, S.A. El-Mogy, A.I. Abou-Kandil, Novel modification of styrene butadiene rubber/acrylic rubber blends to improve mechanical, dynamic mechanical, and swelling behavior for oil sealing applications. Polym. Polym. Compos. **29**(9), S959–S968 (2021). https://doi.org/10.1177/09673911211031351
29. J. Liu, X. Li, L. Xu, P. Zhang, Investigation of aging behavior and mechanism of nitrile-butadiene rubber (NBR) in the accelerated thermal aging

environment. Polym. Test. **54**, 59–66 (2016). https://doi.org/10.1016/j.polymertesting.2016.06.010
30. M. Dridi, S. Hachemi, A.A. Belkadi, Influence of styrene-butadiene rubber and pretreated hemp fibers on the properties of cement-based repair mortars. Eur. J. Environ. Civ. Eng. **27**, 538–557 (2023). https://doi.org/10.1080/19648189.2022.2052968
31. C. Kasprzak, J. Brown, K. Feller, P. Scott, V. Meenakshisundaram, C. Williams, T. Long, Vat photopolymerization of reinforced styrene-butadiene elastomers: a degradable scaffold approach. ACS Appl. Mater. Interfaces **14**(16), 18965–18973 (2022)
32. P. Scott, V. Meenakshisundaram, M. Hegde, C. Kasprzak, C. Winkler, K. Feller, C. Williams, T. Long, 3D printing latex: a route to complex geometries of high molecular weight polymers. ACS Appl. Mater. Interfaces **12**(9), 10918–10928 (2020)